Selective Laser Melting of Density Graded TI6AL4V

Low, Kin Huat; Sun, C. N.; Leong, Kah Fai; Liu, Zhong Hong; Zhang, Dan Qing; Wei, J.

2014

Low, K. H., Sun, C. N., Leong, K. F., Liu, Z. H., Zhang, D. Q., & Wei, J.. (2014). Selective Laser Melting of Density Graded TI6AL4V. Proceedings of the 1st International Conference on Progress in Additive Manufacturing (Pro-AM 2014), 72-77.

https://hdl.handle.net/10356/84259

https://doi.org/10.3850/978-981-09-0446-3_078

SELECTIVE LASER MELTING OF DENSITY GRADED TI6AL4V

K.H. LOW[1,2]

C.N. SUN[1,3], K.F. LEONG[1,2], Z.H. LIU[1,2], D.Q. ZHANG[1,2], J. WEI[1,3]

[1] *SIMTech-NTU Joint Laboratory (3D Additive Manufacturing), Nanyang Technological University, 50 Nanyang Avenue, Singapore 639798*

[2] *NTU Additive Manufacturing Centre, School of Mechanical & Aerospace Engineering, Nanyang Technological University, HW1-01-05, 2A Nanyang Link, Singapore 637372*

[3] *Singapore Institute of Manufacturing Technology, 71 Nanyang Drive, Singapore 638075*

ABSTRACT: Functionally graded materials are generally described as having graded properties due to the usage of two or more materials in the construction of a single part, or through one or more mechanical properties in part design. Selective laser melting allows the fabrication of functionally graded materials through both such designs. Two density graded Ti6Al4V blocks were fabricated via the selective laser melting process, which made use of variance in process parameters and part design toward achieving functional gradient of part density from near full-dense to 10.89% relative density.

INTRODUCTION

Functional gradient refers to the variation of mechanical properties of components as opposed to just homogeneous properties. Functionally graded materials (FGM) realize the concept of functional gradient via both the constitution of multiple materials in the fabrication of a part, giving rise to graded properties which originate from the source materials, as well as integrating one or more mechanical properties across the physical part through component design (Byrd and Birman 2007; Lu, Chekroun et al. 2011). In nature, bio-tissues of living organisms, such as bones, exhibit both traits of functional gradient in terms of material as well as design (Knoppers, Gunnink et al. 2005; Leong, Chua et al. 2008; Oxman, Keating et al. 2011; Mahamood, Akinlabi et al. 2012). In the aerospace industry, FGM are applied to attain both thermal and load bearing capabilities in a single part, due to the high operating temperatures experienced in flight (Cooley 2005; Ho, Kotousov et al. 2007; Natarajan and Manickam 2012). The other applications of FGM include orthopedic implants, composite electrodes for fuel cells and armor composites (Chin 1999; Müller, Drašar et al. 2003; Pompe, Worch et al. 2003).

Bulk FGM fabricated via centrifugal methods, additive manufacturing processes and powder metallurgy enable the fusion of multiple materials in the formation of voluminous FGM (Kieback, Neubrand et al. 2003; Mahamood, Akinlabi et al. 2012). Selective laser melting (SLM), an additive manufacturing technique based on powder metallurgy, is one such method which is capable of producing FGM. The process involves the melting and fusing of powders towards achieving dense parts, which comprises the usage of laser power, directed via an X-Y optical scanner, in scanning and melting individual layers of metal powder. The advantage of the SLM production process includes the ability to form FGM parts via the usage of multiple materials

Proc. of the Intl. Conf. on Progress in Additive Manufacturing
Edited by Chua Chee Kai, Yeong Wai Yee, Tan Ming Jen and Liu Erjia

ISBN: 978-981-09-0446-3 :: doi:10.3850/978-981-09-0446-3_078

(Beal, Erasenthiran et al. 2007). In addition, due to the freeform manufacturing technique involved, complex geometries, which may not be producible by conventional casting or forming methods, allow the formation of parts with functionally graded designs. The functionally graded component formed may allow either varied properties across the span of the component, providing specialized or optimized properties at the required section, or realize weight savings through the usage of lattice or matrix structures in place of solid block designs.

In this paper, SLM was used to fabricate two density graded Ti6Al4V blocks via both the variation of process parameters as well as design of part structure.

EXPERIMENTAL PROCEDURES

The powder used for the SLM process was extra low interstitial (ELI) Ti6Al4V (Grade 23) with particle size of 5 – 40 µm, produced by LPW Technology Ltd via plasma atomization. Powder was assessed to be spherical under scanning electron microscopy using the JEOL JSM-7600F system.

The SLM experiment was performed using the SLM 250 HL system from SLM Solution GmbH, utilizing a Ytterbium Fiber Laser from an IPG YLR-400-WC module. The laser has a wavelength of 1070 nm, with a maximum power of 400W in continuous laser mode and spot size of 80 µm operating in the gaussian beam profile mode.

Two density graded blocks were designed to achieve the effect of functional gradient. The first density graded block was formed with solid sub blocks of known difference in relative density from the introduction of random pores arising from process parameters, as shown in **Table 1**, with layer thickness set at 50 µm and scanned with the chessboard strategy which was rotated 15° between each layer.

Table 1. Process parameters for solid density graded sub blocks

	Laser power (W)	Scanning velocity (mm / s)	Hatch spacing (µm)
Sub solid block 1	120	400	80
Sub solid block 2	177	400	118
Sub solid block 3	42	200	75

The second density graded block was formed with the integration of lattice structures into the design of the sub block, thereby manipulating the relative density of the part. The process parameters for all the lattice sub blocks were as follow: laser power of 120 W, scanning velocity of 400 mm / s, hatch spacing of 80 µm, and powder layer thickness of 50 µm, with the chessboard scanning strategy, rotated 15° between each layer, utilized in the SLM process. This same set of process parameters was also utilized for sub solid block 1, which was chosen for this experiment as it had obtained an average Ti6Al4V part relative density of 99.76%.

The process parameters utilized for sub solid block 1, as well as for the lattice block, were proven to obtain tensile properties of SLM formed Ti6Al4V elaborated in the results and discussion section. The tensile tests were conducted using an Instron 5569 Universal Testing Machine, augmented with an Instron 2630 clip-on extensometer for precise yield stress and strain measurements. The tensile samples were designed according to standard ASTM E8/E8M-11

subsize specimen with length of 100mm, thickness of 6mm and gage length of 25mm. Tensile specimens were processed on the SLM substrate in the X-Y plane, that is, the tensile tests were conducted perpendicular to the samples' build direction. A total of six samples were prepared, with three as built and three heat treated. The heat treatment applied on some of these tensile coupons involved the heating of Ti6Al4V samples at 10°C/min in an argon filled furnace at a flow rate of 20 cubic feet per hour and held at 850°C for 2 hours, followed by furnace cooling till 80°C. This same set of heat treatment was adopted in (Vrancken, Thijs et al. 2012) as it had provided an optimized balance of tensile strength versus elongation of a SLM formed Ti6Al4V part.

EXPERIMENTAL RESULTS AND DISCUSSION

The microstructures of Ti6Al4V blocks formed via the SLM process are as shown in **Figure 1**. The XY plane is characterized by a martensitic microstructure comprising acicular α needles in a Widmanstätten pattern. Columnar prior β grains which grew epitaxially along the building direction were observed on both the XZ and YZ planes, which have similar microstructures due to the rotating chessboard scanning strategy utilized in the build. The anisotropic characteristic of the columnar prior β grain growth illustrates the directional effect of the build direction (Z-axis) on the grain growth direction. The microstructures in **Figure 1** are representative of those belonging to that of the solid block and the lattice block.

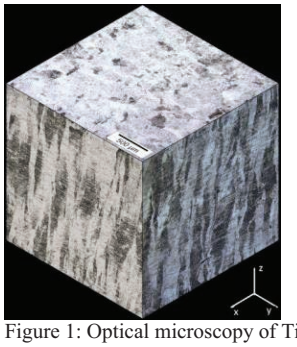

Figure 1: Optical microscopy of Ti6Al4V block fabricated through the SLM process

The SEM of both as built and heat treated Ti6Al4V samples are as shown in **Figure 2**. Coarser α plates were observed for the heat treated samples, which corresponds to the observation in (Vrancken, Thijs et al. 2012). Also, β phase was observed to have grown to be coarser for the heat treated samples.

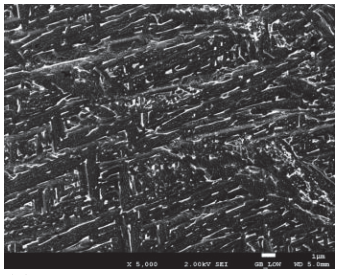

(a)

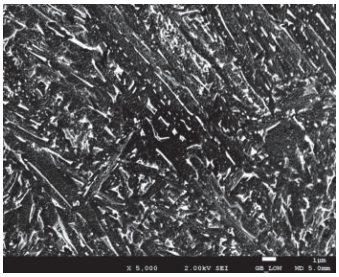

(b)

Figure 2: Scanning electron microscopy of the XY plane of (a) as built and (b) heat treated SLM formed Ti6Al4V, represented by the darker α phase and lighter β phase (5000 X)

Tensile properties of SLM formed Ti6Al4V parts fabricated with process parameters utilized for sub solid block 1 as well as for the lattice block (**Table 1**) are as shown in **Figure 3**, including the samples which underwent heat treatment as well as comparison with the ASTM F3001-13 along the X and Y build directions. The rapid solidification of the SLM process resulted in the formation of a martensitic microstructure, giving rise to the high yield stress and ultimate tensile strength of the as built sample. Also, the ductility of the SLM formed Ti6Al4V part is comparatively lower than that of forged Ti6Al4V due to the fine acicular α phase of the SLM part as compared to the equiaxial α in forged and cast Ti6Al4V (Vrancken, Thijs et al. 2012).

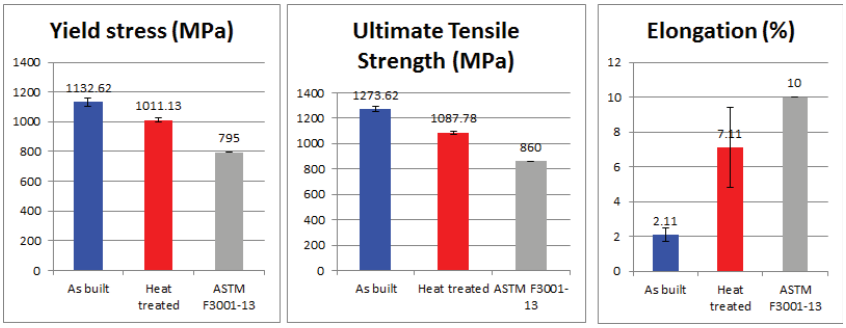

Figure 3: Tensile properties of SLM formed Ti6Al4V part

The tensile properties of SLM formed Ti6Al4V attained in **Figure 3** were based on tensile specimens built in the X-Y plane on the substrate. There has yet to be definite correlations between SLM build directions and the tensile properties of the part built, as differences in tensile results due to difference in build directions have not been significant (Kong, Tuck et al. 2011; Manfredi, Calignano et al. 2013; Rickenbacher, Etter et al. 2013). However, from the comparison of tensile properties of as built samples with that of heat treated samples, the heat treatment process improved the ductility of the samples while trading off their yield stress and ultimate tensile strength (**Figure 3**).

Density of the blocks (**Figure 4** and **Figure 5**) was obtained using Archimedes' principle via utilizing individual sub blocks built specifically for density measurement, which were fabricated with the same geometries and process parameters. For the lattice sub blocks, additional calculations were involved to arrive at the actual lattice density, less the solid border, via the removal of the blocks' border from the density calculation. The dry mass of the lattice sub blocks was measured via the weighing of six individual lattice blocks fabricated with the same process parameters and lattice designs as the lattice block. The volume of the individual solid borders was calculated by measuring the length, width and depth of each border, and multiplied to their respective density to obtain the weight of each border. The resultant weight of the respective lattice was then obtained by subtracting the weight of each border from the weight of each lattice block. Finally, the relative density of each lattice was obtained by dividing the weight of each lattice by the volume of the lattice.

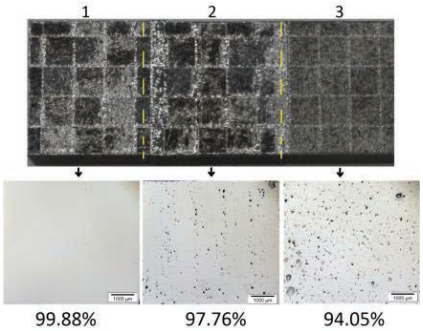

Figure 4: Solid density graded block with the relative densities of sub blocks and the corresponding OM of their porosity

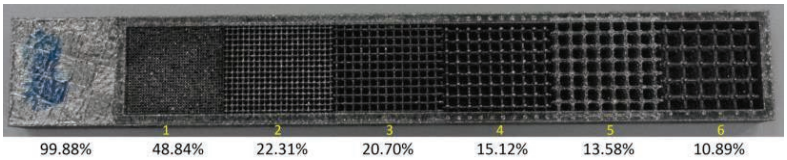

Figure 5: Lattice density graded block with the relative densities of sub blocks

The relative density of the solid block was graded from 99.88% to 94.05% across the length of the block. Likewise, the relative density of the lattice block was graded from 99.88% to 10.89%. For the former, porosity of the respective sub blocks requires prior experimental validation of part relative density, whereas for the latter, porosity of the respective sub blocks could be theoretically calculated through the design of each block. For the solid block, the density gradient of component was attained via usage of different sets of process parameters in the SLM process to create known porosity in each sub block of the component. In contrast, the density gradient for the lattice block was achieved via the introduction of porosity in the design of component. As such, process parameters used in fabricating the solid block could be considered as sub-optimal, as not all sets of process parameters could achieve full part density. Conversely, optimal process parameters could be utilized in fabricating the lattice block as the control of density gradient is via the usage of part design.

As shown in **Figure 5**, the design of the lattice block was an amalgamation of the individual sub lattice blocks, without alignment of the sub lattice block structures. To evaluate mechanical properties, such as compressive or tensile strength, design of the lattice structure could be improved to align the struts of the inter-sub block lattice to enable the transfer of stress from one end of the density graded block to the other. The usage of optimized lattice designs in the Computer Aided System for Tissue Scaffolds (CASTS), employed for the design of biomedical scaffolds, could aid the development of functionally graded structures fabricated via SLM (Sudarmadji, Tan et al. 2011). Also, the usage of individual sub lattice blocks in forming the lattice block had resulted in discrete gradients formed across the interfaces of adjacent sub lattice blocks, giving rise to segmented mechanical properties across the block itself. To improve the gradual transition of mechanical properties from one end of the lattice block to the other, usage of continuous gradient in the design of the component could be adopted instead.

CONCLUSION

Functionally graded Ti6Al4V blocks were fabricated via the SLM process, with graded relative density of 99.88% to 10.89% successfully achieved. The creation of functional gradient via the manipulation of process parameters and part design allows the introduction of known porosity in the fabricated blocks. Future work on FGC could focus on the integration of lattice design to form a continuously linked structure within a lattice block having continuous functional gradient.

REFERENCES

Beal, V., Erasenthiran, P., et al. (2007). "Evaluating the use of functionally graded materials inserts produced by selective laser melting on the injection moulding of plastics parts." Proceedings of the Institution of Mechanical Engineers, Part B: Journal of Engineering Manufacture 221(6): 945-954.

Byrd, L. W. and Birman, V. (2007). "Modeling and analysis of functionally graded materials and structures." Applied Mechanics Reviews 60: 195.

Chin, E. S. C. (1999). "Army focused research team on functionally graded armor composites." Materials Science and Engineering: A 259(2): 155-161.

Cooley, W. G. (2005). Application of functionally graded materials in aircraft structures, DTIC Document.

Ho, S.-Y., Kotousov, A., et al. (2007). FGM (Functionally Graded Material) Thermal Barrier Coatings for Hypersonic Structures-Design and Thermal Structural Analysis, DTIC Document.

Kieback, B., Neubrand, A., et al. (2003). "Processing techniques for functionally graded materials." Materials Science and Engineering: A 362(1–2): 81-106.

Knoppers, G., Gunnink, J., et al. (2005). The reality of functionally graded material products. Intelligent Production Machines and Systems-First I* PROMS Virtual Conference: Proceedings and CD-ROM set, Access Online via Elsevier.

Kong, C.-J., Tuck, C. J., et al. (2011). "High Density TI6AL4V Via SLM Processing: Microstructure and Mechanical Properties."

Leong, K., Chua, C., et al. (2008). "Engineering functionally graded tissue engineering scaffolds." Journal of the mechanical behavior of biomedical materials 1(2): 140-152.

Lu, L., Chekroun, M., et al. (2011). "Mechanical properties estimation of functionally graded materials using surface waves recorded with a laser interferometer." NDT & E International 44(2): 169-177.

Mahamood, R. M., Akinlabi, E. T., et al. (2012). "Functionally Graded Material: An Overview." Lecture Notes in Engineering and Computer Science 2199.

Manfredi, D., Calignano, F., et al. (2013). "From Powders to Dense Metal Parts: Characterization of a Commercial AlSiMg Alloy Processed through Direct Metal Laser Sintering." Materials 6(3): 856-869.

Müller, E., Drašar, Č., et al. (2003). "Functionally graded materials for sensor and energy applications." Materials Science and Engineering: A 362(1): 17-39.

Natarajan, S. and Manickam, G. (2012). "Bending and vibration of functionally graded material sandwich plates using an accurate theory." Finite Elements in Analysis and Design 57: 32-42.

Oxman, N., Keating, S., et al. (2011). Functionally graded rapid prototyping. Innovative Developments in Virtual and Physical Prototyping: Proceedings of the 5th International Conference on Advanced Research in Virtual and Rapid Prototyping.

Pompe, W., Worch, H., et al. (2003). "Functionally graded materials for biomedical applications." Materials Science and Engineering: A 362(1–2): 40-60.

Rickenbacher, L., Etter, T., et al. (2013). "High temperature material properties of IN738LC processed by selective laser melting (SLM) technology." Rapid Prototyping Journal 19(4): 282-290.

Sudarmadji, N., Tan, J., et al. (2011). "Investigation of the mechanical properties and porosity relationships in selective laser-sintered polyhedral for functionally graded scaffolds." Acta Biomaterialia 7(2): 530-537.

Vrancken, B., Thijs, L., et al. (2012). "Heat treatment of Ti6Al4V produced by Selective Laser Melting: Microstructure and mechanical properties." Journal of Alloys and Compounds 541: 177-185.